



日本原子力研究開発機構機関リポジトリ  
Japan Atomic Energy Agency Institutional Repository

Title	Second-order structural transition in $(\text{Ca}_{0.5}\text{Sr}_{0.5})_3\text{Rh}_4\text{Sn}_{13}$
Author(s)	Cheung Y. W., Hu Y. J., Goh S. K., Kaneko Koji, Tsutsui Satoshi, Logg P. W., Grosche F. M., Kanagawa Hibiki, Tanioku Yasuaki, Imai Masaki, Matsumoto Takuya, Yoshimura Kazuyoshi
Citation	Journal of Physics; Conference Series, 807(3), p.032002_1-032002_4
Text Version	Publisher
URL	<a href="https://jopss.jaea.go.jp/search/servlet/search?5056360">https://jopss.jaea.go.jp/search/servlet/search?5056360</a>
DOI	<a href="https://doi.org/10.1088/1742-6596/807/3/032002">https://doi.org/10.1088/1742-6596/807/3/032002</a>
Right	Content from this work may be used under the terms of the Creative Commons Attribution 3.0 licence ( <a href="http://creativecommons.org/licenses/by/3.0/">http://creativecommons.org/licenses/by/3.0/</a> ). Any further distribution of this work must maintain attribution to the author(s) and the title of the work, journal citation and DOI.

# Second-order Structural Transition in $(\text{Ca}_{0.5}\text{Sr}_{0.5})_3\text{Rh}_4\text{Sn}_{13}$

Y W Cheung<sup>1</sup>, Y J Hu<sup>1</sup>, S K Goh<sup>1,\*</sup>, K Kaneko<sup>2</sup>, S Tsutsui<sup>3</sup>,  
P W Logg<sup>4</sup>, F M Grosche<sup>4</sup>, H Kanagawa<sup>5</sup>, Y Tanioku<sup>5</sup>, M Imai<sup>5</sup>,  
T Matsumoto<sup>5</sup>, K Yoshimura<sup>5</sup>

<sup>1</sup> Department of Physics, The Chinese University of Hong Kong, Shatin N.T., Hong Kong, China

<sup>2</sup> Materials Sciences Research Center, Japan Atomic Energy Agency, Tokai, Naka, Ibaraki 319-1195, Japan

<sup>3</sup> Japan Synchrotron Radiation Research Institute (JASRI), SPring-8, Sayo, Hyogo 679-5198, Japan

<sup>4</sup> Cavendish Laboratory, University of Cambridge, J. J. Thomson Avenue, Cambridge CB3 0HE, United Kingdom

<sup>5</sup> Department of Chemistry, Graduate School of Science, Kyoto University, Kyoto 606-8502, Japan

E-mail: skgoh@phy.cuhk.edu.hk

**Abstract.**  $(\text{Ca}_{0.5}\text{Sr}_{0.5})_3\text{Rh}_4\text{Sn}_{13}$  is a member of the substitution series  $(\text{Ca}_x\text{Sr}_{1-x})_3\text{Rh}_4\text{Sn}_{13}$  which has recently been argued to feature a structural quantum critical point at  $x_c = 0.9$ . In the stoichiometric compound  $\text{Sr}_3\text{Rh}_4\text{Sn}_{13}$ , the structural transition at  $T^* \approx 138$  K has been shown to be second-order. Moving towards  $x_c$ , we examine the character of the structural transition in  $(\text{Ca}_{0.5}\text{Sr}_{0.5})_3\text{Rh}_4\text{Sn}_{13}$  (*i.e.*  $x = 0.5$ ,  $T^* \approx 55$  K) using electrical resistivity, heat capacity and X-ray scattering. The absence of the thermal hysteresis in specific heat around  $T^*$ , and the continuous evolution of the superlattice reflection detected by X-ray diffraction are consistent with the scenario that the structural transition associated with a modulation vector  $\mathbf{q} = (0.5 \ 0.5 \ 0)$  in  $(\text{Ca}_{0.5}\text{Sr}_{0.5})_3\text{Rh}_4\text{Sn}_{13}$  remains second-order on approaching the quantum critical point.

## 1. Introduction

$\text{Sr}_3\text{Rh}_4\text{Sn}_{13}$  is a conventional *s*-wave superconductor with a critical transition temperature ( $T_c$ ) of 4.7 K [1, 2, 3]. In addition to the superconducting transition, another second-order phase transition takes place at  $T^* = 138$  K. This high temperature transition has been established to be a structural phase transition between the  $Pm\bar{3}n$  and  $I\bar{4}3d$  space groups above and below  $T^*$ , respectively.  $T^*$  can be suppressed either by applying pressure or by calcium substitution, *i.e.* by forming a  $(\text{Ca}_x\text{Sr}_{1-x})_3\text{Rh}_4\text{Sn}_{13}$  substitution series [1, 3]. If the structural transition remains second order as  $T^* \rightarrow 0$ , a structural quantum critical point can be realized [1, 4].

In the substitution series  $(\text{Ca}_x\text{Sr}_{1-x})_3\text{Rh}_4\text{Sn}_{13}$ ,  $T^*$  can be completely suppressed solely by fine tuning the calcium content, and it has been established that  $T^* \rightarrow 0$  when  $x = x_c \approx 0.9$  [1]. In the vicinity of  $x_c$ , several important observations are noted: (a) Debye temperature is a minimum, (b)  $T_c$  is a maximum, and (c) strong-coupling superconductivity can be stabilized. All these features can be nicely understood in the framework of structural quantum criticality, and



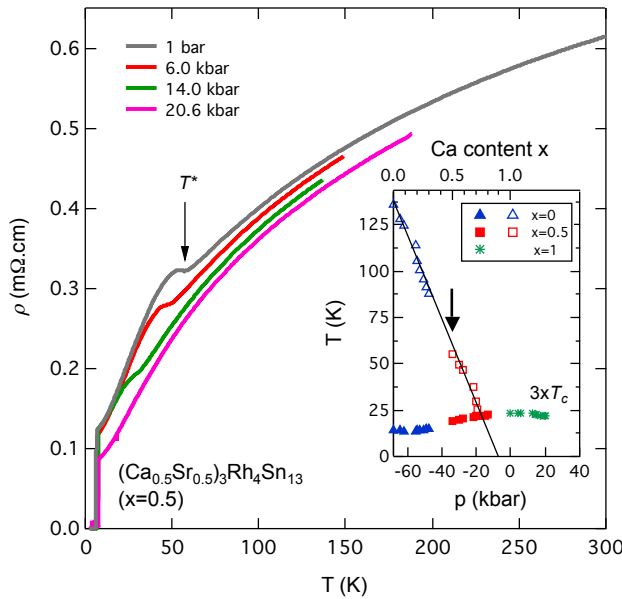


**Figure 1.** Temperature dependence of the electrical resistivity measured at different pressures. The arrow indicates  $T^*$  at ambient pressure. Inset: Universal temperature-pressure phase diagram constructed using  $\text{Sr}_3\text{Rh}_4\text{Sn}_{13}$ ,  $(\text{Ca}_{0.5}\text{Sr}_{0.5})_3\text{Rh}_4\text{Sn}_{13}$ , and  $\text{Ca}_3\text{Rh}_4\text{Sn}_{13}$ . For details, see reference [1].  $\text{Sr}_3\text{Rh}_4\text{Sn}_{13}$  is located at the leftmost edge of the phase diagram. The location of  $(\text{Ca}_{0.5}\text{Sr}_{0.5})_3\text{Rh}_4\text{Sn}_{13}$  is shown by the arrow.

they thus provide strong support for the identification of  $x_c$  as a quantum critical point [1, 3]. In  $\text{Sr}_3\text{Rh}_4\text{Sn}_{13}$  ( $x=0$ ), specific heat data unambiguously proved that the structural transition is second-order [1, 3]. In this article, we move closer towards  $x_c$ , and demonstrate that the  $T^*$  transition remains second-order in  $(\text{Ca}_{0.5}\text{Sr}_{0.5})_3\text{Rh}_4\text{Sn}_{13}$  ( $x = 0.5$ ) using our latest x-ray diffraction data.

## 2. Experimental Details

Single crystals of  $(\text{Ca}_{0.5}\text{Sr}_{0.5})_3\text{Rh}_4\text{Sn}_{13}$  were grown using the Sn-flux method as described elsewhere [5]. Electrical resistivity and heat capacity were measured using Quantum Design's Physical Properties Measurement System. High pressure electrical resistivity was measured using a piston-cylinder pressure cell with Daphne 7373 as the pressure transmitting medium. Superlattice reflection was measured at BL35XU of SPring-8, Japan with a Si(11 11 11) backscattering analyzer on the two-theta arm, which helps to reduce the background. The X-ray energy is 21.747 keV.

## 3. Results and Discussion

The inset to Figure 1 displays the universal temperature-pressure phase diagram constructed earlier [1], with the arrow marking the position of  $(\text{Ca}_{0.5}\text{Sr}_{0.5})_3\text{Rh}_4\text{Sn}_{13}$ . It is therefore more than halfway between  $x = 0$  and  $x_c$ . The main panel of Figure 1 shows the temperature dependence of the electrical resistivity for  $(\text{Ca}_{0.5}\text{Sr}_{0.5})_3\text{Rh}_4\text{Sn}_{13}$  at ambient pressure, 6.0 kbar, 14.0 kbar and 20.6 kbar. In addition to the superconducting transition at low temperature, the structural transition at  $T^* \sim 55$  K can be identified as the hump in the electrical resistivity. When pressure is applied,  $T^*$  decreases rapidly, reaching 46.9 K and 29.7 K at 6.0 kbar and 14.0 kbar, respectively. At 20.6 kbar, the  $T^*$  feature is no longer visible in the electrical resistivity. This confirms the trend that pressure moves the system towards the right hand side of the phase diagram.

In  $\text{Sr}_3\text{Rh}_4\text{Sn}_{13}$ , a pronounced lambda-like jump was detected at  $T^*$  [1, 6], without any thermal hysteresis [1]. In the inset to Figure 2, we display the specific heat data of  $(\text{Ca}_{0.5}\text{Sr}_{0.5})_3\text{Rh}_4\text{Sn}_{13}$  around  $T^*$  collected on warming and on cooling. The specific heat anomaly is significantly weaker here compared with the case of  $\text{Sr}_3\text{Rh}_4\text{Sn}_{13}$ . However, the absence of thermal hysteresis

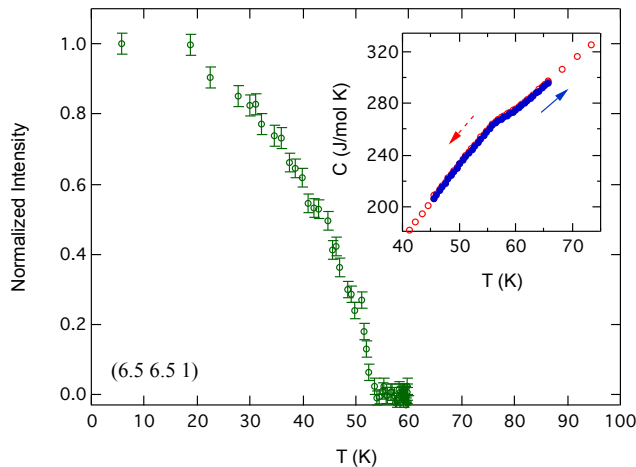


**Figure 2.** Temperature evolution of the X-ray diffraction intensity associated with the superlattice reflection with  $\mathbf{q} = (0.5 \ 0.5 \ 0)$ . (Inset) Temperature dependence of the specific heat in  $(\text{Ca}_{0.5}\text{Sr}_{0.5})_3\text{Rh}_4\text{Sn}_{13}$  around  $T^*$ , collected on cooling (open symbols) and on warming (closed symbols).

is still clear. In the main panel of Figure 2, we present the temperature evolution of the elastic X-ray scattering intensity for  $\mathbf{Q} = (6.5 \ 6.5 \ 1.0)$ . The additional reflection at  $\mathbf{Q} = \mathbf{k} + \mathbf{q}$  below  $T^*$ , where  $\mathbf{k} = (6.0 \ 6.0 \ 1.0)$  corresponds to the Bragg spots in the high temperature ( $T > T^*$ ) phase, is consistent with a modulation vector with  $\mathbf{q} = (0.5 \ 0.5 \ 0)$  (or the  $\mathbf{M}$  point).  $T^*$  determined from the onset of the superlattice reflection is slightly below that obtained from the specific heat data. This difference can be attributed to a slight variation in the calcium content between different samples. From the slope  $dT^*/dx$  (*c.f.* Figure 1 and Ref. [1]), a variation of 0.03 in  $x$  can cause a variation of up to 5 K in  $T^*$ . Finally, the gradual and continuous increase of the diffraction intensities on cooling below  $T^*$  is consistent with the scenario of a second-order phase transition.

#### 4. Conclusion

In summary, we have studied single crystals of  $(\text{Ca}_{0.5}\text{Sr}_{0.5})_3\text{Rh}_4\text{Sn}_{13}$  using electrical resistivity, heat capacity and X-ray diffraction. From the absence of the thermal hysteresis around  $T^*$  in the heat capacity data and the continuous evolution of the superlattice peak intensity at  $(6.5 \ 6.5 \ 1)$ , we conclude that the structural transition in  $(\text{Ca}_{0.5}\text{Sr}_{0.5})_3\text{Rh}_4\text{Sn}_{13}$  is a second-order phase transition with  $\mathbf{q} = (0.5 \ 0.5 \ 0)$ . Similar conclusion has recently been reached in related compounds  $\text{La}_3\text{Co}_4\text{Sn}_{13}$  [7],  $\text{Sr}_3\text{Ir}_4\text{Sn}_{13}$  [6],  $\text{Sr}_3\text{Rh}_4\text{Sn}_{13}$  [6] and  $\text{Ca}_3\text{Ir}_4\text{Sn}_{13}$  [8] from x-ray/neutron diffraction. These data highlights the similarity across different 3-4-13 families in which the notion of structural quantum criticality has been discussed [1, 4, 9].

#### Acknowledgments

The authors acknowledge financial support from Research Grant Council (ECS/24300214), The National Natural Science Foundation of China (No. 11504310), CUHK Direct Grant (No. 3132719), EPSRC of the UK (EP/K012894/1), Grant-in-Aids for Scientific Research (B) (No. 22350029 and 16H04131), and (C) (No. 24540336), and for Challenging Exploratory Research (No. 15K14170) from Japan Society for the Promotion of Science. This experiment was carried out under the approval of JASRI (Proposal No. 2013B1095, 2015B1294 and 2016A1160).

#### References

- [1] Goh S K, Tompsett D A, Saines P J, Chang H C, Matsumoto T, Imai M, Yoshimura K and Grosche F M 2015 *Phys. Rev. Lett.* **114**(9) 097002
- [2] Kuo C N, Tseng C W, Wang C M, Wang C Y, Chen Y R, Wang L M, Lin C F, Wu K K, Kuo Y K and Lue C S 2015 *Phys. Rev. B* **91**(16) 165141

- [3] Yu W C, Cheung Y W, Saines P J, Imai M, Matsumoto T, Michioka C, Yoshimura K and Goh S K 2015 *Phys. Rev. Lett.* **115**(20) 207003
- [4] Klintberg L E, Goh S K, Alireza P L, Saines P J, Tompsett D A, Logg P W, Yang J, Chen B, Yoshimura K and Grosche F M 2012 *Phys. Rev. Lett.* **109**(23) 237008
- [5] Yang J, Chen B, Michioka C and Yoshimura K 2010 *J. Phys. Soc. Jpn.* **79** 113705
- [6] Lue C S, Kuo C N, Tseng C W, Wu K K, Liang Y H, Du C H and Kuo Y K 2016 *Phys. Rev. B* **93**(24) 245119
- [7] Cheung Y W, Zhang J Z, Zhu J Y, Yu W C, Hu Y J, Wang D G, Otomo Y, Iwasa K, Kaneko K, Imai M, Kanagawa H, Yoshimura K and Goh S K 2016 *Phys. Rev. B* **93**(24) 241112(R)
- [8] Mazzone D G, Gerber S, Gavilano J L, Sibille R, Medarde M, Delley B, Ramakrishnan M, Neugebauer M, Regnault L P, Chernyshov D, Piovano A, Fernández-Díaz T M, Keller L, Cervellino A, Pomjakushina E, Conder K and Kenzelmann M 2015 *Phys. Rev. B* **92**(2) 024101
- [9] Ślebarski A, Fijałkowski M, Maška M M, Mierzejewski M, White B D and Maple M B 2014 *Phys. Rev. B* **89**(12) 125111